Unstable manifolds computation for the two-dimensional plane Poiseuille flow*

Pablo S. Casas
Departamento de Matemática Aplicada I. Universidad Politécnica de Cataluña
Diagonal, 647. 08028 Barcelona. Spain
e-mail: pablo@casas.upc.es - Web page: http://www-ma1.upc.es/˜casas

Àngel Jorba
Departamento de Matemática Aplicada y Anlisis. Universidad de Barcelona
Gran Via, 585. 08007 Barcelona. Spain
e-mail: angel@maia.ub.es - Web page: http://www.maia.ub.es/˜angel

Communicated by

Received date and accepted date

Abstract. We follow the unstable manifold of periodic and quasi-periodic solutions in time for the Poiseuille problem, using two formulations: holding constant flux or mean pressure gradient. By means of a numerical integrator of the Navier-Stokes equations, we let the fluid evolve from an initially perturbed unstable solution until the fluid reaches an attracting state. Thus, we detect several connections among different configurations of the flow such as laminar, periodic, quasi-periodic with 2 or 3 basic frequencies, and more complex sets that we have not been able to classify. Those connections make possible the location of new families of solutions, hard to find by means of numerical continuation of curves, and shows the richness of the dynamics of the Poiseuille flow.

1. Introduction

The plane Poiseuille flow is a classic in the theory of hydrodynamic stability. It is named after Jean Léonard Marie Poiseuille (Paris 1797–1869), who was mainly interested in the study of the flow of liquids in small diameter glass capillaries. Since the times of Poiseuille this problem has been the subject of uncountable works, concerning its stability and the transition to turbulence, which still has no satisfactory answer. Among those works Zahn, Toomre, Spiegel, and Gough (1974), using a constant mean pressure gradient, computed travelling waves as steady flows in an appropriate Galilean reference. For the two-dimensional case they found the region in the Re_p-α plane where there exist travelling waves and in turn the instability region of the linear theory. They obtained a surface of the energy of disturbances for each pair Re, α, given rise to an upper and lower branch of solutions. By perturbing these two sets of solutions and following them in time, they estimated their stability and thus they found that the lower branch is unstable and the upper stable, at least to the disturbances employed. Herbert (1976) also obtained periodic secondary flows for constant mean

* This research has been partially supported by funds from the Departamento de Matemática Aplicada I (Universidad Politécnica de Cataluña), the Spanish CICYT grant BFM2000–0623, the Catalan CIRIT grant 2001SGR–70, and DURSI.

pressure gradient in two dimensions using more spectral modes. He pointed out the slow convergence of the Fourier series for those flows. Rozhdestvensky and Simakin (1984) implemented a numerical integrator to simulate the flow over different time intervals. By observing the flow rate and the pressure gradient they obtain secondary flows. They found secondary flows non-periodic in time in two dimensions for long wave-lengths ($\alpha \approx 0.3$) and also in three dimensions for different wave-lengths. Jiménez (1987) proposed to study the existence of bifurcations leading to limit cycles in plane Poiseuille flow as possible early steps in the appearance of disorder. At $Re_Q = 5000$ (always $\alpha = 1.0$) he followed the upper branch of time-periodic orbits and found that for $Re_Q \approx 5000$-6000 the periodic flow shed a limit cycle. The number of Fourier–Chebyshev modes used, varies from 7×33 to 15×65. For $Re_Q > 9000$, the limit cycle becomes disordered and bifurcates into new solutions that include tori and, later, chaos. Jiménez (1990) does full numerical simulation of spatially periodic channels with fairly large longitudinal aspect ratios. He finds travelling waves, one and two frequency tori and chaos for several values of Re_Q and α. Computations were mostly performed using 41×85 Fourier–Chebyshev modes. With this approach he was only able to obtain attracting solutions.

On the contrary Soibelman and Meiron (1991), by means of the vorticity equation, computed steady two-dimensional travelling waves and branches of quasi-periodic solutions which bifurcate from them. They found both stable and unstable solutions for formulations in terms of Re_p and Re_Q, although the number of Fourier modes was not enough to assure convergence. In Casas (2002) the number of modes were increased and there were obtained different qualitative results in the stability and location of the bifurcated quasi-periodic flows.

In the present work we keep studying the dynamics of plane Poiseuille flow, analysing the connection among different configurations of the flow, such as laminar, periodic or quasi-periodic. These solutions were calculated in Casas (2002) where we classified them with the help of dynamical system tools such as the Poincaré section. We are interested in how the fluid evolves and which kind of solution it is conducted to when it starts on an unstable solution, as the ones shown in figures 1 and 2 (see bellow). The various links discovered among different states of the flow allow us to reproduce some results obtained in Jiménez (1987), such us tori with 2 or 3 basic frequencies and more disordered configurations. We have also discovered new families of unstable 2-tori through the connection of unstable manifolds. However their continuation still needs a deeper study.

The organization of this paper is as follows: in § 2, we first formulate the problem and give an overall description of the numerical approach. In § 3 and § 4 are detailed how the disturbance of the unstable flow is constructed and how the connection of its unstable invariant manifold is attained.

2. Problem formulation

We consider the plane Poiseuille flow in dimension 2, where the fluid is confined in a channel of plane parallel walls. The problem is modeled by the incompressible Navier-Stokes equations

$$\frac{\partial \mathbf{u}}{\partial t} + (\mathbf{u} \cdot \boldsymbol{\nabla})\mathbf{u} = -\nabla p + \frac{1}{Re}\Delta \mathbf{u}, \qquad \boldsymbol{\nabla} \cdot \mathbf{u} = 0, \tag{1}$$

together with no-slip and periodic boundary conditions

$$\left.\begin{aligned} u(x, \pm 1, t) = v(x, \pm 1, t) = 0 \\ (u, v, p')(x + L, y, t) = (u, v, p')(x, y, t) \end{aligned}\right\} \qquad x \in \mathbb{R}, \quad y \in [-1, 1], \quad t \geqslant 0, \tag{2}$$

being Re the Reynolds number, $p' = p + 2x/Re$ and $L = 2\pi/\alpha$ (α is the parameter wave number). We have considered the two typical formulations to drive the fluid through the channel: holding constant the total flux or the mean pressure gradient. For each of them we obtain a different definition of $Re = hU_c/\nu$, where h represents half of the channel length, U_c the velocity of the dimensional laminar flow (steady solution of (1)-(2) with parabolic profile) in the centre of the channel, and ν the kinematic viscosity. If we fix a constant flux Q, then $U_c = 3Q/(4h)$, On the other hand for a constant pressure gradient G, we get $U_c = Gh^2/(2\mu)$. Therefore

$$Re_Q = \frac{3Q}{4\nu}, \qquad Re_p = \frac{Gh^3\rho}{2\mu^2},$$

corresponds to the Reynolds numbers when we keep Q as a constant flux or G as a constant mean pressure gradient respectively. The fluid is supposed of constant density ρ and viscosity μ. The numerical approximation is detailed in Casas (2002). Roughly, it employs Fourier and Chebyshev spectral discretizations of velocities and pressure in the periodic and transversal directions respectively. The temporal variable is approximated by means of finite differences.

In figures 1 and 2 we represent bifurcating curves of periodic and quasi-periodic flows obtained numerically in Casas (2002) using $N = 8$ and $M = 70$ spectral modes in the x and y spatial directions respectively. For the temporal discretization the time step has been prescribed to $\Delta t = 0.02$. This values of discretization are kept throughout the paper. Two different values for α are considered, namely $\alpha = 1.02056$ and $\alpha = 1.1$. Each point of those curves corresponds to the amplitude A (distance to the laminar flow in L_2-norm) of the flow (periodic or quasi-periodic in time) for the given value of Re. It is also marked on the curves the different stability regions, together with several Hopf bifurcations. In figure 2 at Re_{Q1}, the Hopf bifurcation of periodic flows give rise to a family of quasi-periodic solutions with 2 basic frequencies, whose stability is also presented. The main load of the computations has been carried out in parallel in a Beowulf cluster of PCs.

3. Unstable invariant manifolds of periodic flows

As Rand (1982) shows, time-periodic solutions of Poiseuille flow with boundary conditions (2), can be observed as stationary solutions in a certain moving frame of reference. Consequently we study the stability of those flows by means of the linearization of the discretized version of (1)–(2). We have selected several time-periodic flows for $\alpha = 1.02056$ and $\alpha = 1.1$, for both cases of Re_p and Re_Q. In order to approximate unstable invariant manifolds, we have considered the two simplest cases of unstable periodic solutions, namely the ones that have one real unstable eigenvalue and the remaining ones stable, or a couple of complex conjugate unstable eigenvalues and the remaining ones stable. The lower branch of periodic flows in figures 1 and 2 belong to the first group. In the case of constant pressure, the arc of the upper branch before Re_{p1} (but a small range beyond the minimum Re_p) and after Re_{p2} for $Re_p < 14000$, correspond to the second group. On the other hand, for Re_Q, only the arc between Re_{Q1} and Re_{Q2} belongs to the second group.

For each periodic flow, $u^p(x, y, t)$, of those two groups, we have studied its unstable manifold and which new state of the fluid they are connected to. By means of the Jacobian matrix (the linearization of the discretized version of (1)–(2)) computed to analyze the stability, we can obtain the eigenvector $w \in \mathbb{C}^K$ (being K the dimension of the discretized system) associated with the unstable eigenvalue. The perturbed flow $u^p + rw$ for $|r| \ll 1$ is thus a first order approximation of the unstable manifold of u^p, which in turn is an attracting manifold. Using the numerical integrator of (1)–(2), we have followed the temporal evolution of $u^p + rw$ until an attracting state is reached. Likewise, in the case that u^p has only one real unstable eigenvalue, we have considered two ways of escaping from u^p according to $r > 0$ or $r < 0$, because we obtain different attractors in each case. When there is a couple of complex conjugate eigenvalues, we have chosen an arbitrary direction in the plane generated by the real and imaginary parts of w: we have not detected changes in the attractor when this direction is varied.

The different configurations obtained for several values of Re_p, Re_Q and α are summarized in table 1. The attractors presented in this table for the cases with one real unstable eigenvalue, are obtained in one direction of the unstable manifold. On the opposite direction the attractor is the laminar solution, except for a few cases where we have found the same attractor in both directions. For $\alpha = 1.1$ these occur at $Re_Q = 5822.$ and for $\alpha = 1.02056$ at $Re_p = 5772$, and $Re_Q = 4405, 5462, 5772$.

For the case of Re_p and $\alpha = 1.02056$, the lower branch is connected with the laminar flow for $Re_p \lesssim 4722$, and with the stable periodic solution on the upper branch for $4766 \lesssim Re_p \lesssim 5772$. For the case of Re_p, $\alpha = 1.1$, the connection of the lower branch is with the laminar flow for $Re_p \lesssim 3802$, with a periodic flow for $3885 \lesssim Re_p \lesssim Re_{p2}$, with a 2-torus for $Re_{p2} \lesssim Re_p \lesssim 9500$, and with different configurations for $Re_p \gtrsim 9500$. For Re_Q, $\alpha = 1.1$, the lower branch is connected with a periodic solution for $Re_Q \leqslant Re_{Q1}$, with a 2-torus for $Re_{Q1} \leqslant Re_Q \lesssim 7950$, with a 3-torus for $7950 \lesssim Re_Q \lesssim 8500$, and with unknown sets

Table 1. Attractors of the flow to which is connected the unstable manifold of periodic solutions on the upper and lower branch of the amplitude curve of figures 1 and 2. The attractors that we have not been able to classify are show as *unkn*. The temporal evolution is presented in figures 3–6 for values of Re marked with '*' in the table.

UPPER BRANCH											
$\alpha = 1.02056$				$\alpha = 1.1$				$\alpha = 1.02056$		$\alpha = 1.1$	
Re_p	attract.	Re_p	attract.	Re_p	attract.	Re_p	attract.	Re_Q	attract.	Re_Q	attract.
4638	laminar	8688	2-torus	3803	laminar	9832	2-torus	5462	2-torus	5264	2-torus
4654	laminar	9067	2-torus	3816	laminar	10388	2-torus	5712	2-torus	5402	2-torus
4680	laminar	9478	2-torus	3835^*	laminar	10990	2-torus	5991	2-torus	5601	2-torus
6952	2-torus	9921^*	2-torus	7268	2-torus	11638	2-torus	6299	2-torus	5801	2-torus
7184	2-torus	10398	2-torus	7615	2-torus			6634	2-torus	6069	2-torus
7438	2-torus	10912	2-torus	7991	2-torus			6997	2-torus	6321	2-torus
7713	2-torus			8398	2-torus					6589	2-torus
8012	2-torus			8839	2-torus					6682	2-torus
8336	2-torus			9316	2-torus					6776	2-torus

LOWER BRANCH											
$\alpha = 1.02056$		$\alpha = 1.1$				$\alpha = 1.02056$		$\alpha = 1.1$			
Re_p	attract.	Re_p	attract.	Re_p	attract.	Re_Q	attract.	Re_Q	attract.	Re_Q	attract.
4636	laminar	3802	laminar	9489	2-torus	4405	laminar	3658	periodic	7359	2-torus
4649	laminar	3885	periodic	9589	unkn.	4487	periodic	3694	periodic	7639	2-torus
4689	laminar	3969	periodic	10513	2-torus	4556	periodic	3816	periodic	7995	3-torus
4722	laminar	4172	periodic	11078	laminar	4668	periodic	4020	periodic	8389^*	3-torus
4766	periodic	4570	periodic	11375	2-torus	4814	periodic	4559	periodic	8682^*	unkn.
4821	periodic	4872	periodic			5004	periodic	4611	periodic	9045	unkn.
4890	periodic	5272	periodic			5462	2-torus	4814	periodic	9363^*	unkn.
4975	periodic	5789	periodic			5602	2-torus	5101^*	2-torus	9589	unkn.
5079	periodic	6397	periodic			5687	2-torus	5500	2-torus	9848	unkn.
5205	periodic	6917	periodic			5772	2-torus	5822^*	2-torus	10139	unkn.
5361	periodic	7813	2-torus					6049	2-torus	10390	unkn.
5554	periodic	8192	2-torus					6499	2-torus	10746	unkn.
5772	periodic	8642	2-torus					6791	2-torus	11096	unkn.
		9094	2-torus					7097	2-torus	11395	unkn.

for $Re_Q \gtrsim 8500$. In this case, for $Re_Q \geqslant Re_{Q1}$ the perturbed unstable periodic flow is first connected with the periodic solution on the upper branch and then it is directed to the final attractor.

The upper branch is connected with the laminar flow for $Re_p \leqslant Re_{p1}$, and with a 2-torus for $Re_{p2} \leqslant Re_p \leqslant Re_{p3}$, for $\alpha = 1.02056$ and, $\alpha = 1.1$, being Re_{p3} the next Hopf bifurcation after Re_{p2}. For the case of Re_Q, $\alpha = 1.1$, the upper branch is also connected with a 2-torus for $Re_{Q1} \leqslant Re_Q \leqslant Re_{Q2}$.

As a summary of table 1 we could say that the final attractor is the stable periodic solution when it exists. Otherwise the attractor can be laminar for Re before the appearance of stable periodic flows, or a stable 2-torus bifurcated from the upper branch. For Re such that the 2-torus is unstable, the attractor is a 3-torus and other configurations of unknown sets.

In figures 3–6 we present the evolution of the perturbed periodic flow for several simulations. On those figures we plot the projection of the discrete velocity on the plane of 2 coordinates (956 and 210 out of $K = 1156$, to be precise) when the flow crosses an appropriate Poincaré section (see Casas, 2002, for details) Σ_1. For instance, on Σ_1 the evolution of a stable periodic flow is represented by a single constant point on those projections, the laminar flow by coordinates $(0, 0)$, and a stable quasi-periodic flow with 2 basic frequencies by a closed curve. Surface levels of stream function and vorticity of the flow of figure 6(b), for $Re_Q = 9363$, are plotted as a reference of the physical situation in figure 7.

4. Unstable invariant manifolds of quasi-periodic flows

In the case of constant flux the bifurcation diagram of periodic flows is qualitatively different from that of constant pressure, as is shown in figures 1 and 2. For Re_Q and there is a change of stability at the minimum Reynolds Re_{Q0} of the curve of amplitudes, but no new bifurcations are born there. The first Hopf bifurcation occurs at the point labeled Re_{Q1} in figure 2. At this point the family of periodic solutions bifurcates to a family of quasi-periodic flows.

As in the case of periodic flows, quasi-periodic solutions with 2 basic frequencies are reducible to periodic if the observer moves in the stream direction at a suitable speed c (see Rand, 1982). By using this property we can compute periodic flows as fixed points of the Poincaré map P_c built on Σ_1. The quasi-periodic solutions found from Re_{Q1} are stable for $Re_{Q1} < Re_Q \lesssim 7950$ if $\alpha = 1.1$ and $Re_{Q1} < Re_Q \lesssim 8070$ if $\alpha = 1.02056$. At $Re_Q \approx 7950$, $\alpha = 1.1$ and $Re_Q \approx 8070$, $\alpha = 1.02056$ the branch of quasi-periodic solutions loses stability to give rise to a family of attracting tori of 3 basic frequencies at a new Hopf bifurcation.

For each unstable 2-torus, $u^q(x, y, t)$, from this Hopf bifurcation, we approximate the linear part of the map P_c by means of extrapolated finite differences. Then we perturb u^q in the direction of the most unstable eigenvectors of the linear part of P_c, associated to two complex conjugate eigenvalues of modulus greater than one. We follow the temporal evolution of this perturbed flow until an attracting state is reached. For $\alpha = 1.1$ and $Re_Q \lesssim 9000$ the attracting flow seems to be a 3-torus, but for greater Re_Q the solution becomes apparently disordered. A completely analogous scenario is achieved for $\alpha = 1.02056$. The main simulations carried out are summarized in table 2, where we show the connections of the unstable manifold corresponding to the unstable 2-tori for $Re_Q \gtrsim 8070$ and $Re_Q \gtrsim 7950$ according to $\alpha = 1.02056$ or $\alpha = 1.1$ respectively. In figures 8–12 we show the temporal evolution for some values of Re_Q presented in table 2.

Finally it is worthwhile to mention the new family of 2-tori found as a continuation of the disordered flow in figure 12(a). This is taken as initial condition using $Re_Q < 9096$. Once the flow becomes stabilized we use it again as initial condition for a smaller Re_Q. The picture of this procedure is depicted in figures 13–16. In figure 16(b) we observe, as the end of this continuation, a 2-torus which turns out to be different from the bifurcated family arisen at Re_{Q1}. Thus, due to the connections of the unstable manifolds, we have found another family of flows not available by means of continuation of the already computed branches. The bifurcating branch that this flow belongs to is still a work in progress.

Table 2. Attractors of the flow to which is connected the unstable manifold of quasi-periodic solutions for Re_Q and $\alpha = 1.1, 1.02056$. The temporal evolution of the flow until the attracting solution is reached is presented in figures 8–12 for Re marked with '*' in the table.

$\alpha = 1.02056$					
Re_Q	attractor	Re_Q	attractor	Re_Q	attractor
8098*	3-torus	8418	3-torus	8701	possible 3-torus
8206	3-torus	8496	possible 3-torus		
8309	3-torus	8600	possible 3-torus		

$\alpha = 1.1$					
Re_Q	attractor	Re_Q	attractor	Re_Q	attractor
7953	3-torus	8322*	3-torus	9005*	possible 3-torus
7975	3-torus	8486	3-torus	9096*	unknown
8043	3-torus	8623	3-torus	9204*	unknown
8157	3-torus	8767	3-torus		
8278	3-torus	8894*	possible 3-torus		

5. Conclusions

The present work is devoted to the numerical study of the connection among different configurations of plane Poiseuille flow. The main part of the computations is carried out by the numerical integrator of the Navier–Stokes equations formulated in terms of velocity and pressure. The connection of the unstable manifold of unstable periodic flow and unstable 2-tori is basically attained with attracting solutions in the studied families of periodic and quasi-periodic flows, or with more complex states, such as 3-tori or more disorder sets, for greater values of Re.

As future work, it would be of interest the study Liapunov exponents for those strange attracting sets that have not been able to classify. Not of least importance is the origin of the new family of 2-tori discovered through unstable manifolds.

References

Alavyoon, F., Henningson, D. S., and Alfredsson, P. H. (1986). Turbulent spots in plane Poiseuille flow – flow visualization. *Phys. Fluids*, 29:1328–1331.

Allgower, E. L. and Georg, K. (1990). *Numerical Continuation Methods*, volume 13 of *Springer Series in Computational Mathematics*. Springer-Berlag.

Canuto, C., Hussaini, M. Y., Quarteroni, A., and Zang, T. A. (1988). *Spectral methods in fluid dynamics*. Springer-Verlag.

Carlson, D. R., Widnall, S. E., and Peeters, M. F. (1982). A flow visualization study of transition in plane Poiseuille flow. *J. Fluid Mech.*, 121:487–505.

Casas, P. S. (2002). *Numerical study of Hopf bifurcations in the two-dimensional plane Poiseuille flow*. PhD thesis, Universidad Politécnica de Cataluña. http://www-ma1.upc.es/˜casas/research.html.

Drissi, A., Net, M., and Mercader, I. (1999). Subharmonic instabilities of Tollmien-Schlichting waves in two-dimensional Poiseuille flow. *Phys. Rev. E*, 60(2):1781–1791.

Ehrenstein, U. and Koch, W. (1991). Three-dimensional wavelike equilibrium states in plane Poiseuille flow. *J. Fluid Mech.*, 228:111–148.

Herbert, T. (1976). Periodic secondary motions in a plane channel. In *Proc. 5th Intl. Conf. on Numerical Methods in Fluid Dynamics*, volume 59 of *Lecture Notes in Physics*, pages 235–240. Springer.

Jiménez, J. (1987). Bifurcations and bursting in two-dimensional Poiseuille flow. *Phys. Fluids*, 30 (12):3644–3646.

Jiménez, J. (1990). Transition to turbulence in two-dimensional Poiseuille flow. *J. Fluid Mech.*, 218:265–297.

Marsden, J. E. and McCracken, M. (1976). *The Hopf bifurcation and its applications*, volume 10 of *Applied Mathematical Sciences*. Springer-Verlag, New York. With contributions by P. Chernoff, G. Childs, S. Chow, J. R. Dorroh, J. Guckenheimer, L. Howard, N. Kopell, O. Lanford, J. Mallet-Paret, G. Oster, O. Ruiz, S. Schecter, D. Schmidt and S. Smale, Applied Mathematical Sciences, Vol. 19.

Nishioka, M. and Asai, M. (1985). Some observartions of the subcritical transition in plane Poiseuille flow. *J. Fluid Mech.*, 150:441–450.

Orszag, S. A. and Patera, A. T. (1983). Hydrodynamic stability of shear flows. In Iooss, G., Helleman, R. H., and Stora, R., editors, *Chaotic behavior of deterministic systems (Les Houches, 1981)*, volume XXXVI, pages 621–662. North-Holland, Amsterdam.

Perko, L. (1998). *Differential equations and dynamical systems*. Springer-Verlag, New York, second edition.

Pugh, J. D. and Saffman, P. G. (1988). Two-dimensional superharmonic stability of finite-amplitude waves in plane Poiseuille flow. *J. Fluid Mech.*, 194:295–307.

Rand, D. (1982). Dynamics and symmetry predictions for modulated waves in rotating fluids. *Arch. Rat. Mech. Anal.*, 79:1–37.

Rozhdestvensky, B. L. and Simakin, I. N. (1984). Secondary flows in a plane channel: their relationship and comparison with turbulent flows. *J. Fluid Mech.*, 147:261–289.

Saffman, P. G. (1983). Vortices, stability, and turbulence. *Ann. N. Y. Acad. Sci.*, 404:12–24.

Soibelman, I. and Meiron, D. I. (1991). Finite-amplitude bifurcations in plane Poiseuille flow: two-dimensional Hopf bifurcation. *J. Fluid Mech.*, 229:389–416.

Zahn, J.-P., Toomre, J., Spiegel, E. A., and Gough, D. O. (1974). Nonlinear cellular motions in Poiseuille channel flow. *J. Fluid Mech.*, 64:319–345.

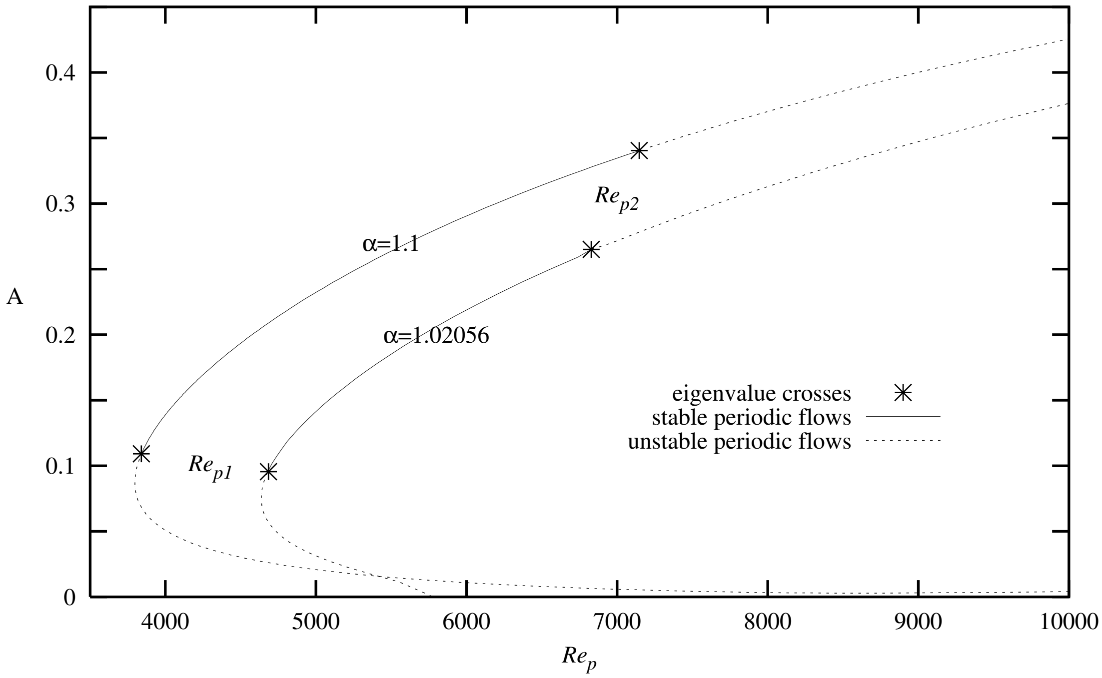

Figure 1. Bifurcating curves of amplitudes for periodic flows based on Re_p for $\alpha = 1.02056$ and $\alpha = 1.1$. The '*' on each curve corresponds to Hopf bifurcations labeled as Re_{p1} and Re_{p2}. They divide the different regions of stability to superharmonic disturbances. Stable solutions are traced by a continuous line, meanwhile the unstable ones are plotted with a discontinuous line.

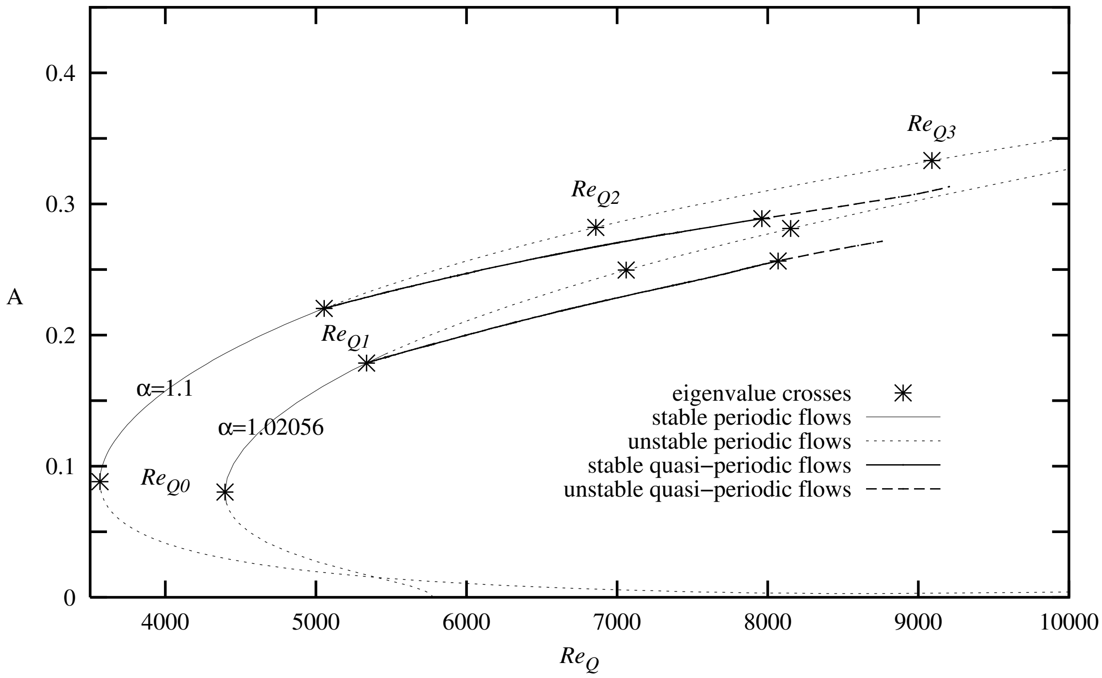

Figure 2. Analogous of figure 1 based on Re_Q. The point labeled as Re_{Q0} is just a change of stability in the periodic solutions but not a bifurcation point, whereas three Hopf bifurcations labeled as Re_{Q1}, Re_{Q2}, and Re_{Q3} are presented on the upper branch. In this case there are also included the bifurcated branches of quasi-periodic flows at Re_{Q1}. These branches have also a Hopf bifurcation where there is a change of stability in the quasi-periodic flows.

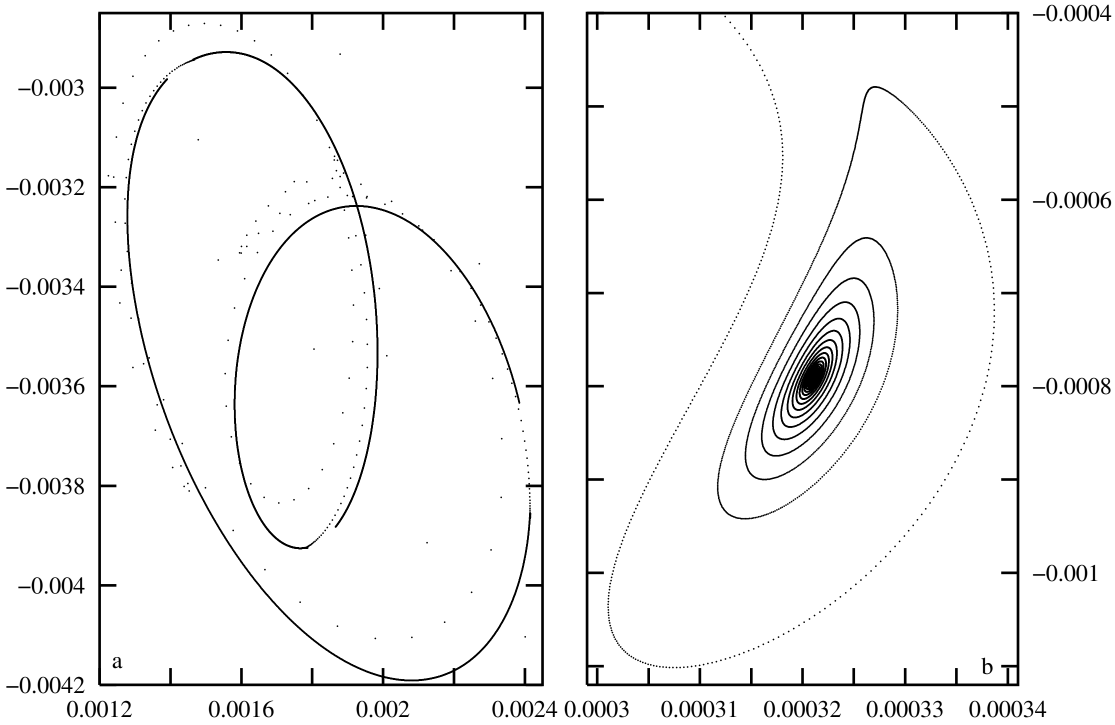

Figure 3. (a) The perturbed unstable periodic flow on the upper branch for $Re_p = 9921$, $\alpha = 1.02056$, is attracted by a 2-torus, which is traced starting from three different points in a continuous way: the curve is plotted not closed intentionally to remark this effect. The integration time on the plot is roughly $262{,}000$ time units. (b) Analogous of (a) for the periodic solution on the upper branch for $Re_p = 3835$, $\alpha = 1.1$, which influenced by the near Hopf bifurcation, initially spirals while decreases amplitude and finally falls to the laminar solution (not shown on the graph). The integration time on this graph was around $175{,}000$ time units.

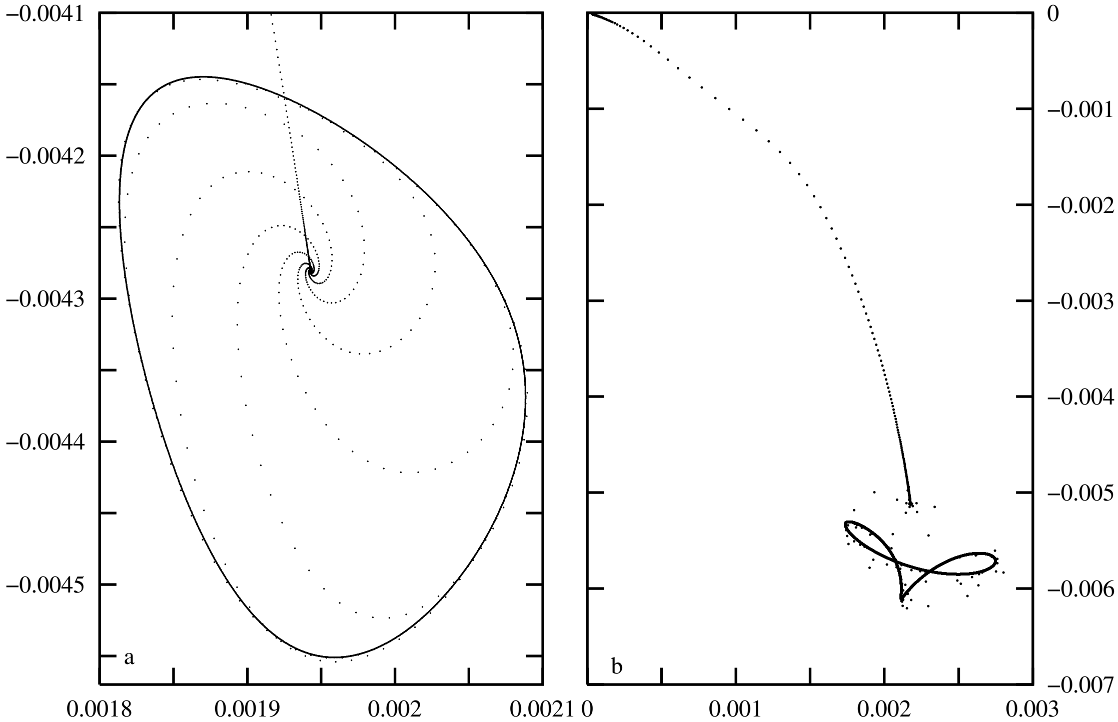

Figure 4. (a) Final steps of the evolution of the perturbed unstable periodic flow on the lower branch for $Re_Q = 5101$, $\alpha = 1.1$. The fluid is first attracted by the unstable periodic flow on the upper branch, a point in the centre of the figure, and then it is driven to a attracting 2-torus. The integration time plotted is around $57{,}000$ time units. (b) Analogous of (a) for a solution on the lower branch for $Re_Q = 5822$, $\alpha = 1.1$, which is represented on the figure close to $(0, 0)$. The fluid is first taken to the unstable periodic flow on the upper branch which finally is attracted by a 2-torus. The integration time on the figure is about $195{,}000$ time units.

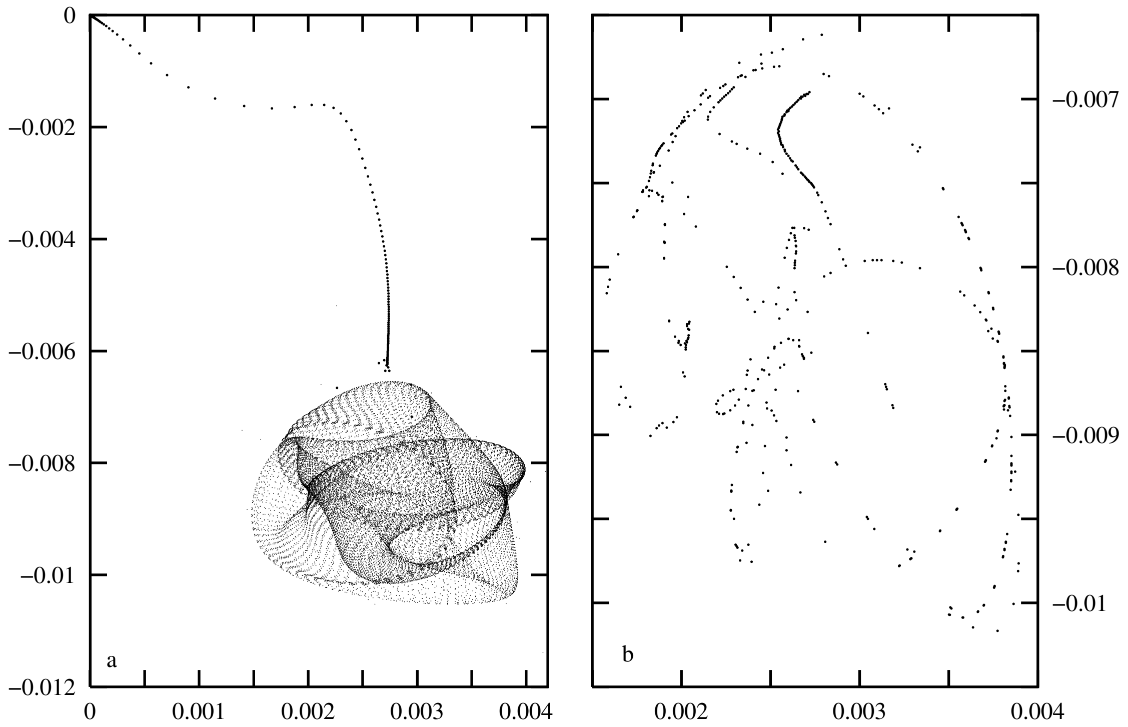

Figure 5. (a) Flow that starts from the perturbed unstable periodic solution on the lower branch for $Re_Q = 8389$, $\alpha = 1.1$. The flow is first directed to the unstable periodic flow on the upper branch and then attracted by a 3-torus. The integration time on the figure is about $322{,}000$ time units. (b) Same flow as (a) but only plotted when it also crosses a second Poincaré section Σ_2. We observe several closed curves, which seem to indicate that the attracting flow is a 3-torus. The integration time on the figure is about $7{,}111{,}000$ time units.

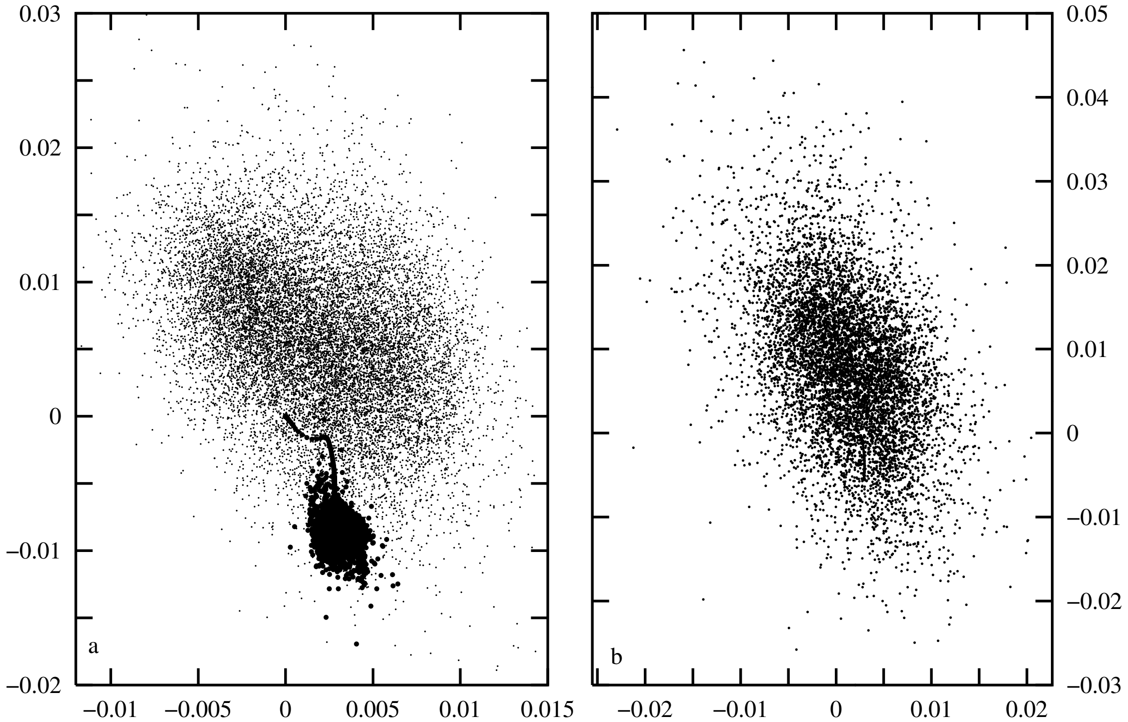

Figure 6. (a) Flow that starts from the perturbed unstable periodic solution on the lower branch for $Re_Q = 8682$, $\alpha = 1.10$. The flow is attracted by a strange set plotted in bigger dots, which is unstable and finally drives the fluid to another strange set. The integration time on the figure is about $245{,}000$ time units. (b) Analogous of (a) for a solution on the lower branch for $Re_Q = 9363$, $\alpha = 1.10$. The flow is attracted by an apparently strange set. The integration time on the figure is about $115{,}000$ time units.

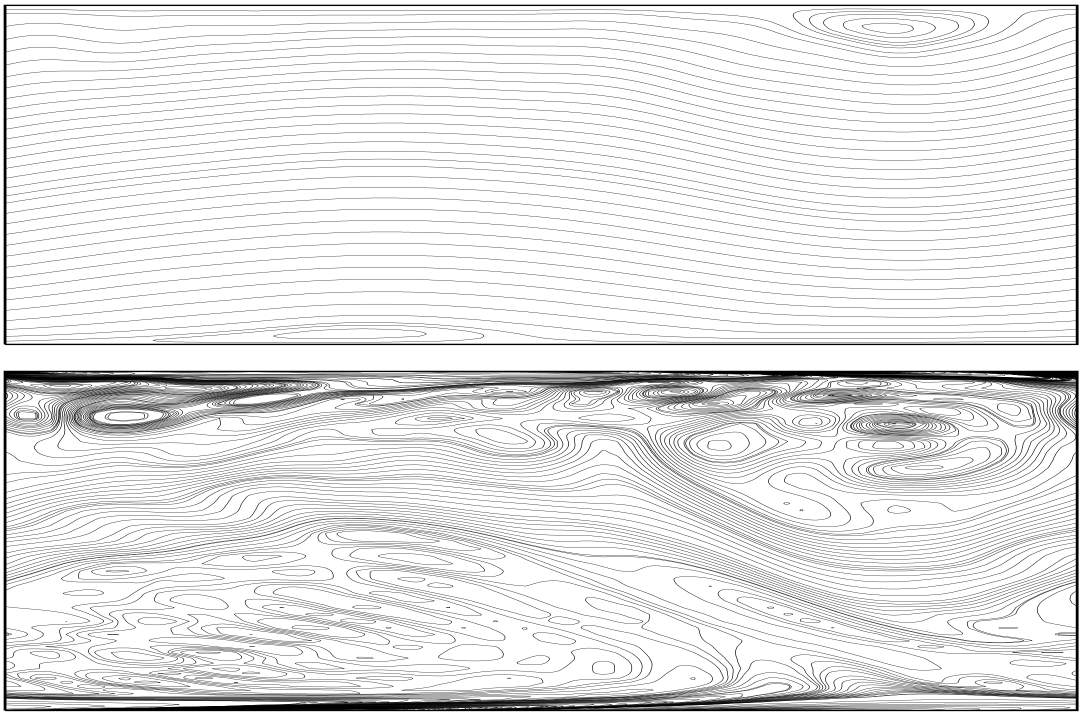

Figure 7. Surface levels of stream function and vorticity respectively in $[0, L] \times [-1, 1]$ for the strange flow for $Re_Q = 9363$ of figure 6(b) at an arbitrary time instant.

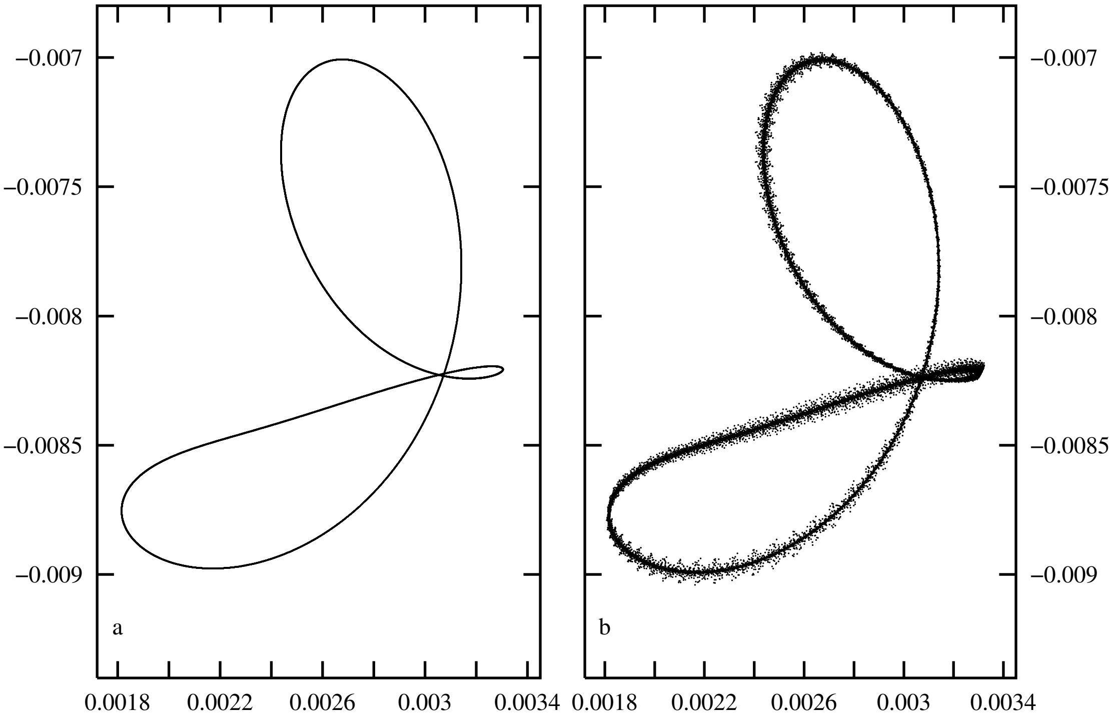

Figure 8. (a) An stable 2-torus on Σ_1. The parameters are $Re_Q = 7940$, $\alpha = 1.1$. The integration time on the figure is about $146{,}000$ time units. (b) Analogous of (a) for $Re_Q = 7948$, $\alpha = 1.1$. We observe in this case that the initial 2-torus is unstable and is attracted by a 3-torus: check figure 9(a). The integration time on the figure is about $513{,}000$ time units.

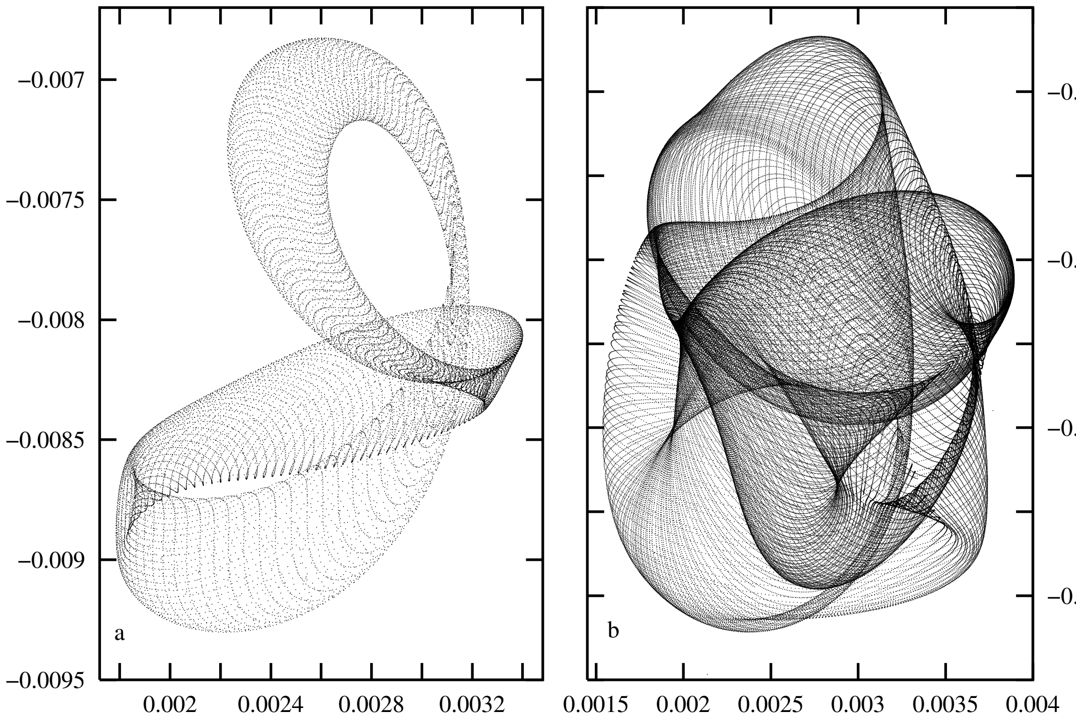

Figure 9. (a) Final attractor for the perturbed unstable 2-torus for $Re_Q = 7948$, $\alpha = 1.1$ of figure 8(b), which turns out to be a 3-torus. The total integration time is of the order of $294{,}000$ time units. (b) Evolution of the perturbed 2-torus for $Re_Q = 8322$, $\alpha = 1.1$, which is attracted by a nearly resonant 3-torus, as can be observed. The total integration time is of the order of $2{,}108{,}000$ time units.

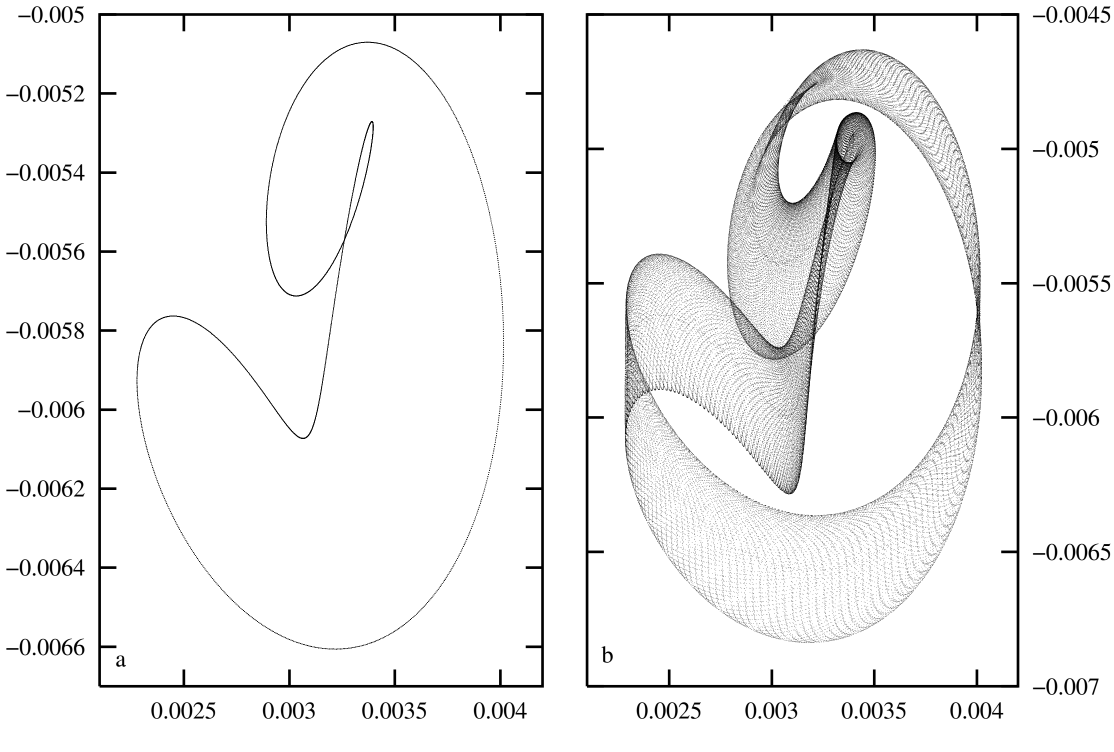

Figure 10. (a) An stable 2-torus on Σ_1 for $Re_Q = 8068$, $\alpha = 1.02056$. The integration time on the figure is about $123{,}000$ time units. (b) Analogous of (a) for $Re_Q = 8098$, $\alpha = 1.02056$. We observe in this case that the initial 2-torus is unstable and is attracted by a 3-torus. The integration time on the figure is about $1{,}753{,}000$ time units.

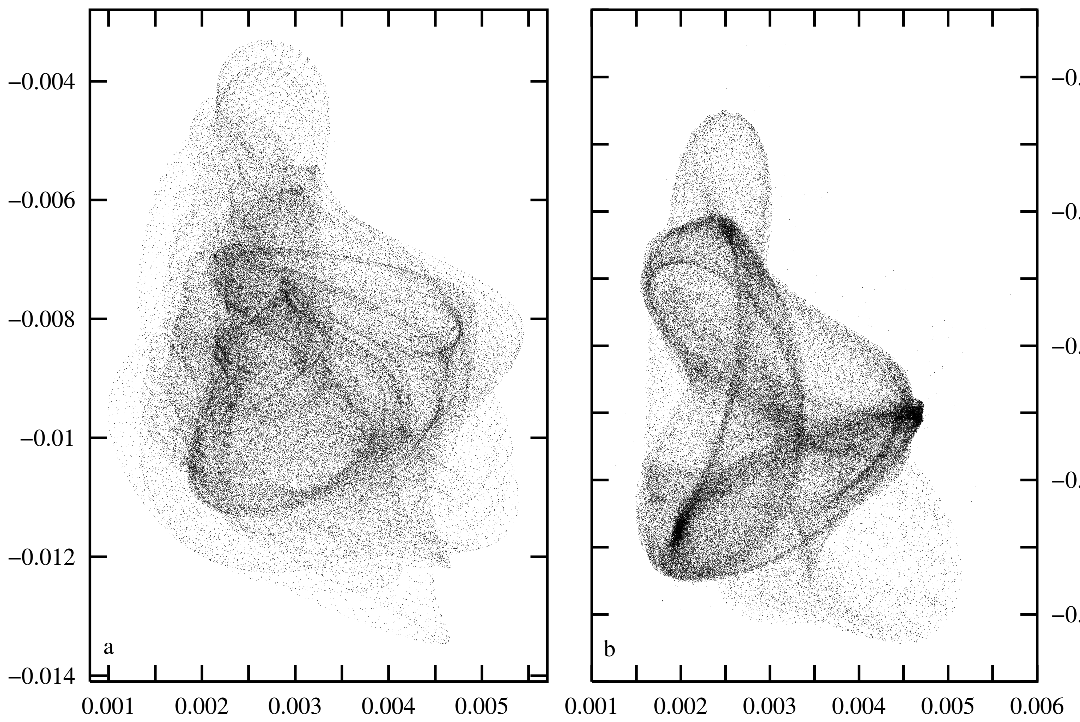

Figure 11. (a) Evolution of the perturbed 2-torus for $Re_Q = 8894$, which is attracted by a set that reminds a 3-torus. The total integration time is of the order of $2{,}110{,}000$ time units. (b) Evolution of the perturbed 2-torus for $Re_Q = 9005$, which is attracted again by a set that reminds a 3-torus. The total integration time is about $2{,}114{,}000$ time units.

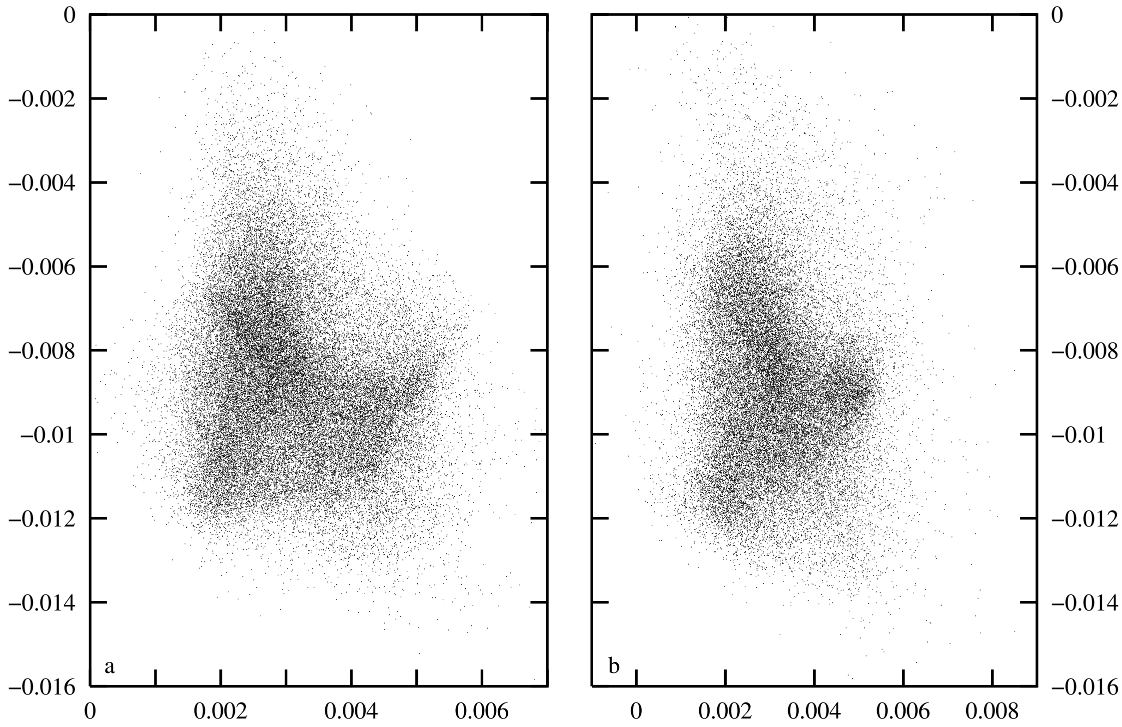

Figure 12. (a) Evolution of the perturbed 2-torus for $Re_Q = 9096$, $\alpha = 1.1$, which is attracted by an apparently strange set. The total integration time is of the order of $592{,}000$ time units. (b) Evolution of the perturbed 2-torus for $Re_Q = 9204$, $\alpha = 1.1$, which is attracted by an apparently strange set. The total integration time is about $463{,}000$ time units.

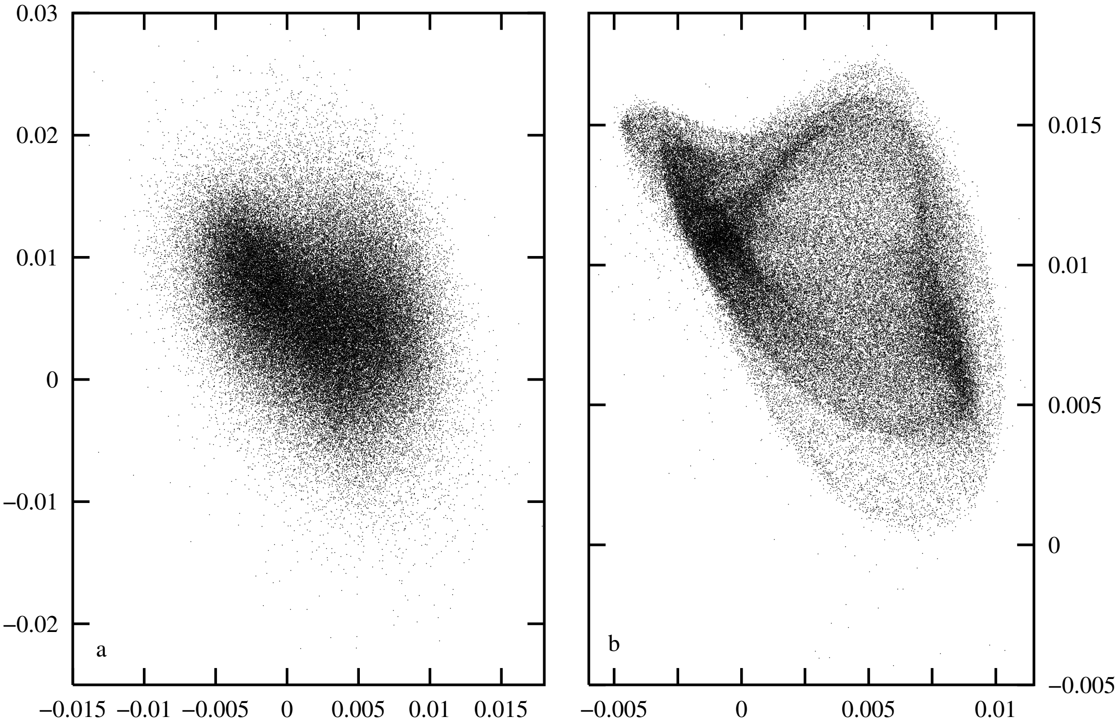

Figure 13. (a) Apparently attracting strange set for $Re_Q = 8500$, $\alpha = 1.1$ obtained as the continuation of the attracting set of figure 12(a) by simply decreasing Re_Q. We remark that we have also obtained an attracting 3-torus for $Re_Q = 8500$. The total integration time is of the order of $1{,}500{,}000$ time units. (b) Continuation for $Re_Q = 7900$, $\alpha = 1.1$, of the solution of (a) attracted by an apparently strange set where we can observe certain order. The total integration time is about $1{,}486{,}000$ time units.

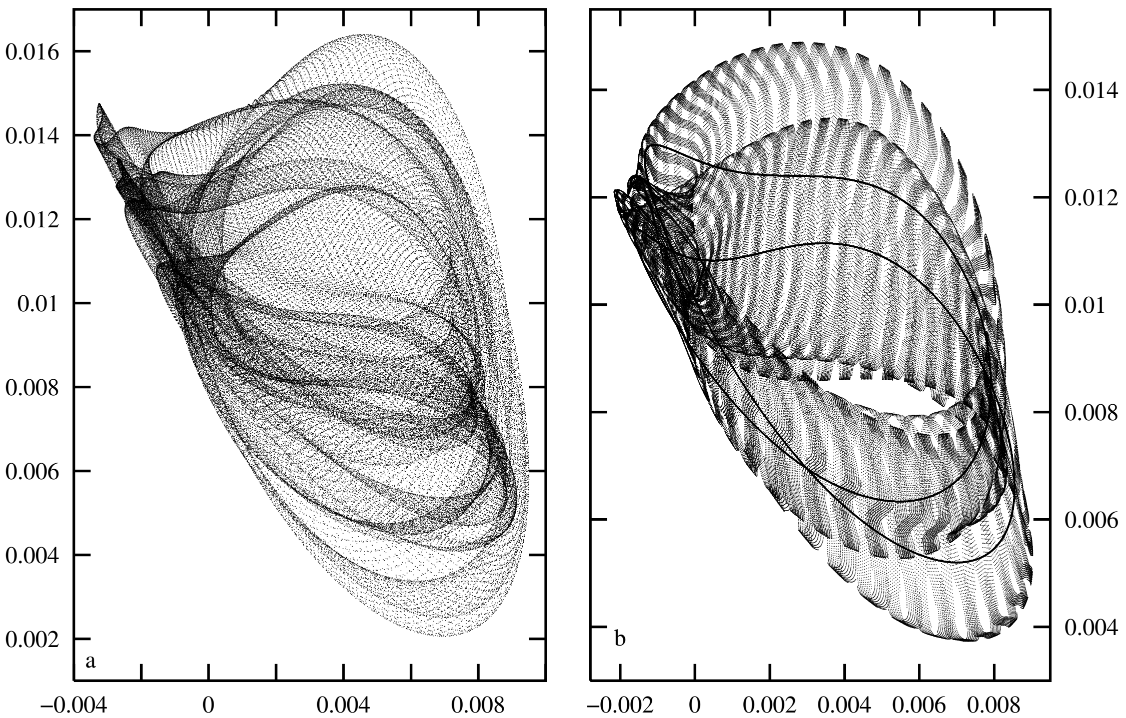

Figure 14. (a) Continuation for $Re_Q = 7800$, of the solution of figure 13(b). We observe in this case a more ordered flow. The total integration time is of the order of $1{,}785{,}000$ time units. (b) The attractor of (a) is taken as initial condition using $Re_Q = 7681$. The total integration time is of the order of $1{,}703{,}000$ time units.

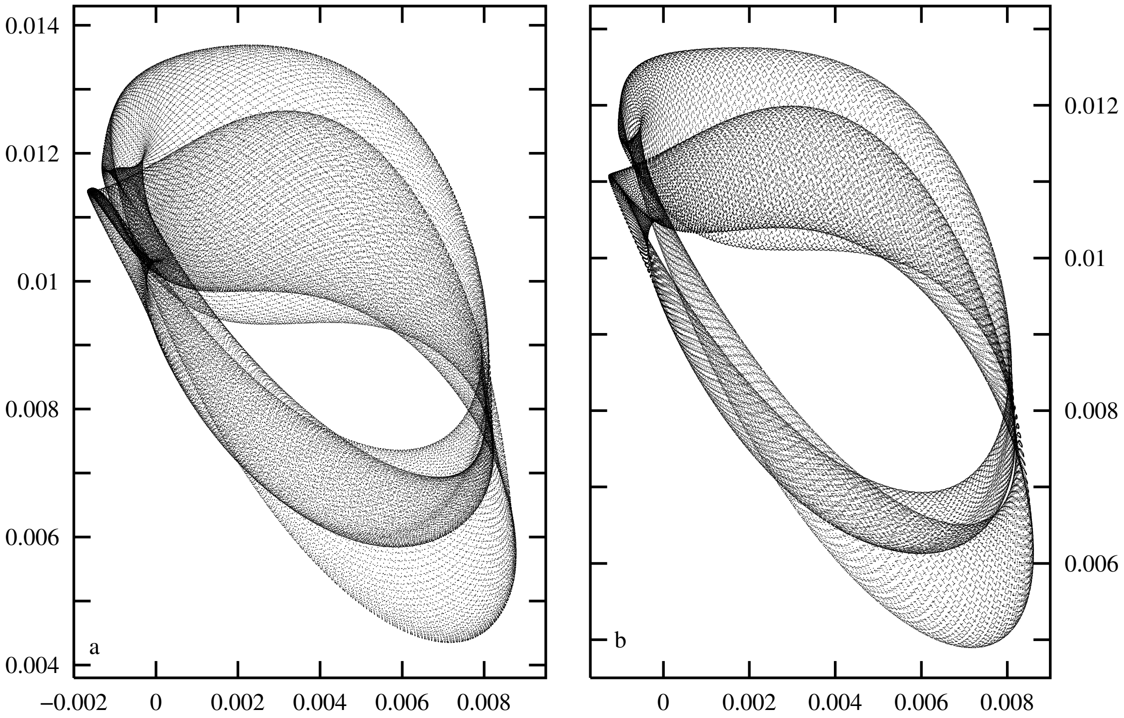

Figure 15. (a) Continuation for $Re_Q = 7650$, of the solution of figure 14(b). The attractor is 3-torus. The total integration time is of the order of $1{,}173{,}000$ time units. (b) Continuation of (a) for $Re_Q = 7640$. The total integration time is of the order of $1{,}144{,}000$ time units.

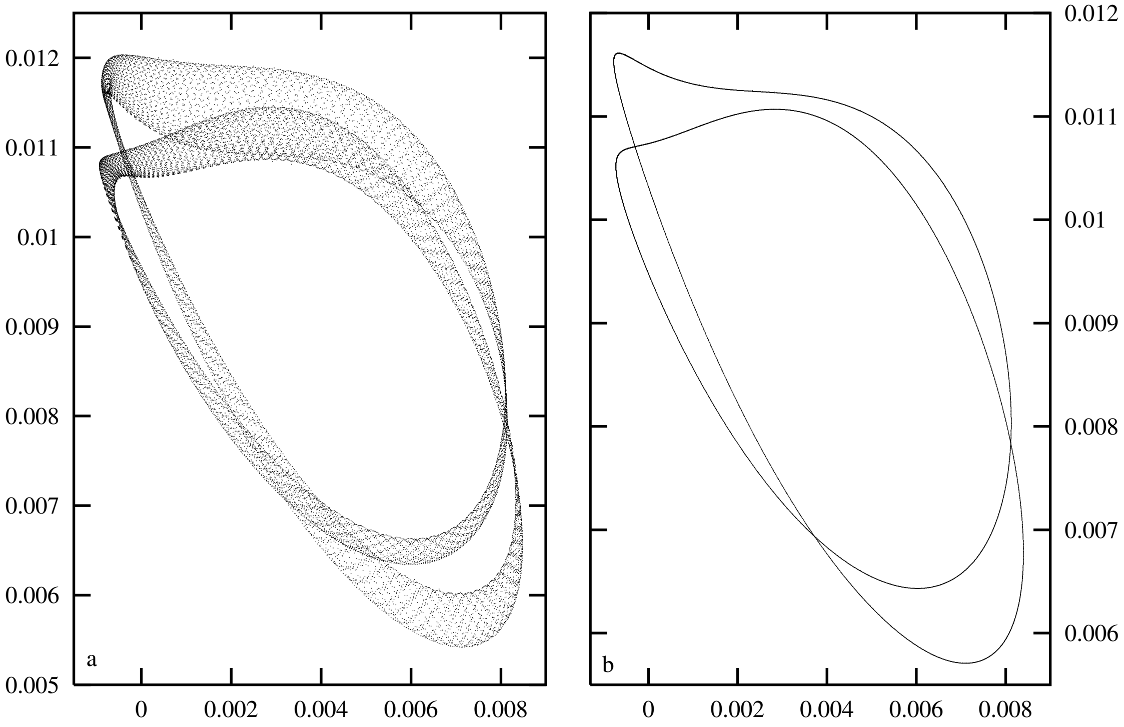

Figure 16. (a) Continuation for $Re_Q = 7637$, of the 3-torus of figure 15(b) which is again attracted by a 3-torus. The total integration time is of the order of $259{,}000$ time units. (b) Continuation of (a) for $Re_Q = 7636$ which is finally attracted by a 2-torus, different from the obtained in the bifurcated branch in figure 2. The total integration time is of the order of $111{,}000$ time units.